

# AC Loss Measurement and Validation of an HTS Soldered Stack Cable for Accelerator Magnets

M. Duda , D. Sotnikov , D. Araujo , B. Auchmann , A. Brem , H. Garcia Rodrigues, T. W. Hanhart, A. Kario , J. Kosse , S. Otten , and A. Ballarino 

**Abstract**—This work explores the use of a double-pancake coil for validating electromagnetic numerical models of HTS cables. We present a cost-effective and rapid production method using 3D-printed plastic formers. High-temperature superconducting (HTS) REBCO tapes are a promising solution for high-field magnets, particularly in accelerator applications, due to their ability to maintain superconducting properties in high magnetic field and high critical current density. One of the most effective ways to utilize HTS tapes is through straight soldered stack cables, which offer excellent packing efficiency in racetrack coil geometries—ideal for Block and Common-coil dipole magnet configurations. Measurements were performed in self-field conditions in liquid nitrogen, with AC current applied at frequencies up to 20 Hz. The current was increased in steps of 5 A of peak current, reaching a maximal of 100 A—below the critical current of the tested samples. For each frequency, the AC loss dependence on peak current showed a smooth trend, while AC losses per cycle remained independent of frequency. The validation process involved finite element method (FEM) modeling, using  $J_c(B)$  interpolation from experimental data, ensuring high accuracy. Both single REBCO tapes and soldered face-to-face cables were analyzed and compared to models of different modelling depth. The computational model matched the measured results with an accuracy within 10%. These findings provide a foundation for further research on the practical application of HTS straight soldered stack cables in high-field accelerator magnets.

**Index Terms**—HTS, superconducting cables, AC loss, superconducting coils.

## I. INTRODUCTION

THE development of next-generation accelerator magnets is driving researchers toward significantly higher magnetic fields, up to 20 T [1]. Achieving these field strengths requires the adaptation and improvement of existing superconducting cable technologies. Among high-temperature superconductors (HTS), REBCO materials are particularly attractive due to their ability to maintain superconductivity under very high magnetic fields. As a result, many research groups are exploring REBCO tapes and cables for use in magnet coils [2].

Received 13 October 2025; revised 13 December 2025; accepted 25 January 2026. Date of publication 6 February 2026; date of current version 23 March 2026. (Corresponding author: M. Duda.)

M. Duda, D. Sotnikov, D. Araujo, A. Brem, H. Garcia Rodrigues, and J. Kosse are with Paul Scherrer Institut PSI, CH-5234 Villigen, Switzerland (e-mail: [michal.duda@psi.ch](mailto:michal.duda@psi.ch)).

B. Auchmann and A. Ballarino are with 2 CERN, CH-1211 Geneva, Switzerland.

T. W. Hanhart, A. Kario, and S. Otten are with the University of Twente, 7500 AE Enschede, The Netherlands.

Color versions of one or more figures in this article are available at <https://doi.org/10.1109/TASC.2026.3661477>.

Digital Object Identifier 10.1109/TASC.2026.3661477

However, no single REBCO cable design has emerged as the perfect solution. Several promising concepts are under investigation, including the transposed Conductor-On-Round-Core (CORC) cable [3], the two-layer STARcable [4], and the Roebel cable [5], which adopts Rutherford-type geometry for REBCO tapes. Each cable type has distinct advantages but also presents significant challenges, particularly in modeling their electromagnetic behavior and AC losses, that play significant role for dipole magnet operation.

The Swiss Accelerator Research and Technology (CHART) initiative is focused on the research and development of robust magnets for the Future Circular Collider (FCC) dipole. Following the 2020 Update of the European Strategy for Particle Physics and in the context of this initiative, PSI proposed the development of a subscale stress-managed common coil magnet, with insulated HTS cable, based on soldered stack of REBCO and copper tapes.

The straight soldered REBCO tapes stack cable offers an excellent packing factor for racetrack coil geometries compared to round wires and closely matches the geometry of low-temperature superconductor (LTS) Rutherford cables ( $\sim 4$  mm wide), enabling performance comparisons. Importantly, this cable is simpler to manufacture and especially well-suited to 2D finite element method (FEM) modeling, making it ideal for early-phase technology validation.

The main goal of this work was to evaluate the performance of a face-to-face soldered REBCO tape stack in a coil configuration and to validate a finite-element model (FEM) for predicting its AC losses. To accomplish this, we fabricated and tested several small pancake coils and compared the measured AC losses with the results from FEM simulations. The key test specimen was a cable consisting of two 4-mm REBCO tapes soldered face-to-face, representing the straight stack configuration for future REBCO accelerator magnet designs. The coils wound with a single REBCO tape were used to validate the FEM model for cases that have already been well characterized in the literature.

As part of the initial development phase, we prioritized quick prototyping and straightforward geometry. Both pancake and layer-wound solenoid coils are well-suited for 2D axisymmetric modeling, but pancakes were selected due to their flat geometry and the fact that they do not require tape twisting—unlike layer-wound solenoids.

The coils were tested at the University of Twente, which offers a validated setup using dual lock-in amplifiers and a four-quadrant power supply capable of delivering peak currents

up to 200 A. This current limit informed the pancake coil design to ensure measurable AC losses. In total, three double-pancake coils were produced using different REBCO cable configurations. One coil, made from a single 4-mm tape, was damaged during fabrication. The remaining two coils were successfully tested, and the measured AC losses aligned well with FEM model predictions.

## II. OBJECT OF RESEARCH

### A. Cables

Due to time limit we had, we prepared samples from three cable types:

- Single 4-mm wide tape;
- Two 4-mm tapes soldered face-to-face (referred to as a straight soldered REBCO stack);
- Single 12-mm wide tape.

Many studies previously validated AC losses computation models for single insulated tape in configuration of a single REBCO tapes, pancake coils winding [6] and racetrack coils [7], which helped validate our computational methods for single tape pancakes.

The 12-mm wide tape serves as a benchmark for comparison with the narrower tapes and supports future studies.

The 4-mm face-to-face soldered stack is a commercial product that we previously procured as a complete cable [8]. It consists of two REBCO tapes with a 40- $\mu\text{m}$  Hastelloy substrate and a 5- $\mu\text{m}$  copper shell surrounding the cable. The two tapes are soldered together and encapsulated with SnPb 60/40 solder, resulting in a total cable thickness of 130  $\mu\text{m}$ .

The single 4-mm and double 4-mm (face-to-face) cables by our plan allow direct comparison under identical total conductor volume at the same current and the same engineering  $J_c$ .

All tapes were supplied from Faraday Factory Japan [8]. Critical current density data,  $J_c(B, \theta)$ , were taken from the Wellington University database [9].

### B. Coil Design

Initial attempts with single-pancake coils revealed problems with the central turn. Heat generated by copper current leads or solder joints near the center significantly affected the first turn critical current. Since this turn is located in the region of highest magnetic field, the impact on performance was considerable.

Using long REBCO tape to form the central connection [10] introduces twisting in the region of highest field or requires the tape to pass perpendicularly through the magnetic field—both ways decay critical current and create bottle neck of the coil.

To mitigate these issues, we adopted a double-pancake configuration (Fig. 1), in which both current leads are located in low-field regions. This arrangement minimizes heat input from resistive contacts, avoids field misalignment at central turns, and simplifies manufacturing.

Three criteria we used for that coils are:

- Quick and easy to produce;
- Low cost;
- High reproducibility.

PLA 3D printing was used to fabricate the coil formers. PLA maintains mechanical robustness in liquid nitrogen and keeps

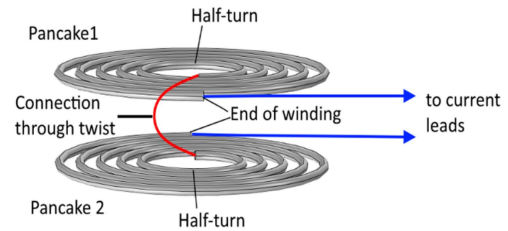


Fig. 1. Double-pancake schematic view.

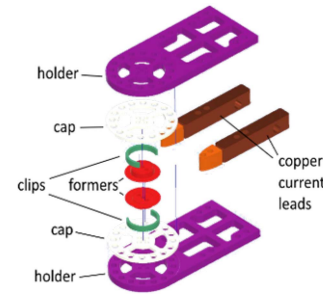


Fig. 2. Key-components of double-pancake coil.

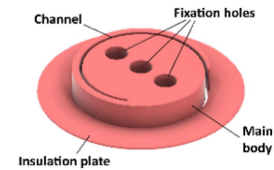


Fig. 3. Double-pancake former for 4-mm cables.

the shape. Printing of all plastic components (Fig. 2) took 2–8 hours depending on coil size.

Current leads were the only machined components, that required additional equipment of workshop. They made from 12 mm square cross-section area copper blocks, with a 5 cm length pre-tin surface for tape soldering.

### C. Coil Production

These coils were designed for testing in liquid nitrogen. For turn-to-turn insulation, we used commercially available 50  $\mu\text{m}$  paper masking tape, which provides sufficient dielectric strength ( $>1$  kV/mm for liquid nitrogen [11]) and thermal stability up to 200°C—suitable for short-time voltage taps soldering. It is easy to coat, cut, and makes thin and flexible REBCO tapes more robust.

The coil former consists of two identical 3D-printed parts (Fig. 3) and includes the following features: holes for fixation to secure the former during winding, a cable channel that guides the cable and defines the twist pitch between the pancakes, insulation plates that form an insulating layer between the pancakes, and the main body, which defines the winding diameter and height of the coil.

The winding process begins by placing the former (i.e., the two connected parts) at the center of the insulated tape through the cable channel. The cable is then carefully laid along the channel, ensuring its edges do not extend beyond the top surface



Fig. 4. Double-pancake winding process.

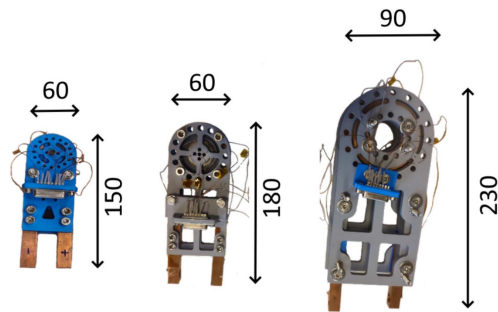


Fig. 5. Three produced double-pancake coils: left - blueBerry (single 4-mm tape); middle - greyBerry4d (face-to-face 4-mm soldered stack); right - greyBerry12 (single 12-mm tape).

TABLE I  
DOUBLE PANCAKE COILS

	Twisted turn diameter, mm	Inner diameter, mm	Outer diameter, mm	Number of turns
blueBerry	17	20	30	28
greyBerry4d	17	20	30	14
greyBerry12	57	60	70	20

of the main body. The channel width must be large enough to accommodate, both the cable itself, ensuring a proper fit inside the channel, and the twisting of the first turn, allowing smooth and secure placement without excessive tension or deformation.

The simplest winding method (Fig. 4) involves the following steps: 1) pull a small section of cable from the spool; 2) rotate the clips to secure the cable; 3) repeat in small steps, ensuring uniform winding and consistent tension.

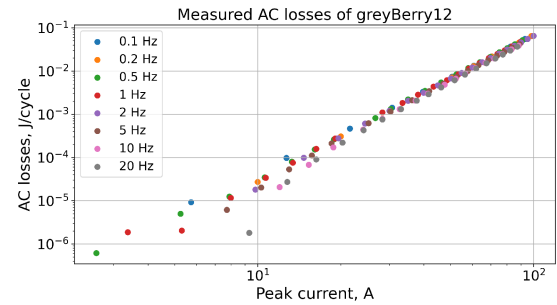
Voltage taps were soldered during winding using flattened copper wires. All voltage taps were connected to D-sub connector socket.

#### D. Coils for Test

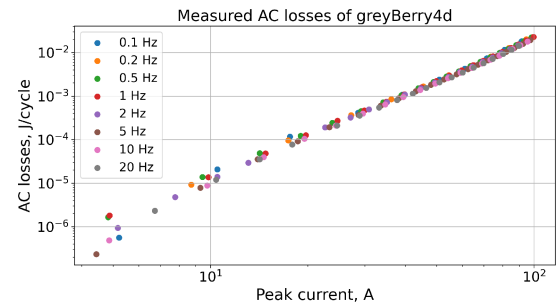
Three coils were produced (Fig. 5): blueBerry (single 4-mm tape), greyBerry4d (face-to-face 4-mm soldered stack), and greyBerry12 (single 12-mm tape). The number of turns and other dimensional characteristics presented in Table I. The number of turns was chosen to ensure a valid comparison of AC losses between single-tape and double-tape soldered stack cables.

### III. MEASUREMENT

In the first test, the blueBerry coil showed unexpectedly high voltage 1 mV at just 25 A DC in liquid nitrogen that points to



(a)



(b)

Fig. 6. Measured AC losses per cycle of: (a) greyBerry12, (b) greyBerry4d.

possible damage during production or handling. Therefore, only greyBerry4d and greyBerry12 were used for final analysis.

#### A. Instrumentation

At the University of Twente, losses are measured using two lock-in amplifiers [12]. One channel measures the phase of the current, while the other measures the phase of the voltage. The phase shift is then determined as the output, enabling the AC loss measurements.

To measure AC losses using an AC signal of known period ( $T$ ), it is necessary to record the RMS values of both current ( $I_{rms}$ ) and voltage ( $U_{rms}$ ) across the coil, along with the phase shift ( $\theta$ ) between them that lock-in amplifier returns as value. Together with the period, this information is sufficient to calculate the AC losses using (1) [13]:

$$W_{coil} = I_{rms} \cdot U_{rms} \cdot T \cdot \cos(\theta). \quad (1)$$

#### B. Results

AC loss measurements were carried out across a frequency range of 0.1 Hz to 20 Hz, with peak currents reaching up to 100 A. Selected voltage taps for measurement were placed outside the coil close the current leads to capture signals from the full coil length while excluding the influence of the leads themselves. The measured parameters included the RMS values of current and voltage at selected voltage taps, along with phase shift data obtained from two lock-in amplifiers.

For peak currents above 20 A, AC losses exhibited a linear dependence on frequency. However, the energy loss per cycle remained constant across frequencies, aligning well with model predictions for the REBCO soldered stack cable (see Fig. 6(a)).

The highest measured losses for greyBerry4d coil were approximately 0.3 W, or 25 mJ per cycle.

Identical measurements were conducted on the greyBerry12 coil. Its per-cycle AC losses were similar to those of the greyBerry4d coil, though the fluctuations in measured losses extended up to 15 A—compared to 10 A in greyBerry4d. The plot of normalized per-cycle energy losses versus frequency (see Fig. 6(b)) confirms the consistency and accuracy of the measurement method.

For critical current ( $I_c$ ) measurements, the available lab equipment at the University of Twente supported a stair-step current profile rather than a continuous linear ramp. The  $I_c$  and  $n$ -value of the cables gotten by V-I curve fitting by power-law [14] function with known lengths of cable in each pancake for criterion  $E_c = 1 \mu\text{V/cm}$ . The greyBerry4d coil critical current values for both the full coil and the individual pancakes were consistent, ranging between 146A and 150A. However, the twisted central half-turn showed a lower  $I_c$  than expected. This reduction is attributed to the higher magnetic field value closer to bore (inner half-turn has lower diameter as presented in Table I) and misalignment between the magnetic field and the REBCO layer surface due to slight twisting of the cable. Length of half-turn connection is small to compare to full coil length, and we assumed AC losses are relatively small due to measurements done at current significantly less than  $I_c$ .

A similar measurement procedure was applied to greyBerry12 coil, but with fewer data points. In this case, the critical current of the central twist was significantly lower than that of the full coil—194 A versus 245 A (maximal applied current was 225 A due to low value of central twist, and  $I_c$  of pancake gotten by fitting function). This may result from two factors: 1) stronger magnetic field effects at the twist, where the field is not optimally aligned with the tape surface; 2) possible mechanical degradation caused by the twisting process. Maximum applied current of 225A, much higher than the 150A applied to the greyBerry4d coil, which may have further stressed the tape.

#### IV. MODELLING

Computation of AC losses done by 2D axisymmetric FEM with Comsol Multiphysics software [15]. We used H-A formulation [16], [17] with H-formulation applied to all current-carrying domains including REBCO layers and metal layers of REBCO tape, and A-formulation for non-conducting domains.

We initially ran simulations using the critical current density values directly from the Robinson database via interpolation. However, the computed results were slightly higher than the experimental measurements. To improve the match between the model and experimental data, we introduced scaling factors of 0.8 and 0.9 for the current density. The 0.8 scaling factor provided the best agreement, closely aligning the simulation with the measured values (see Fig. 7(a)). When applied to the greyBerry4d coil, this scaling factor also produced an excellent match between measured and calculated AC losses (Fig. 7(b)), with an error of less than 10%.

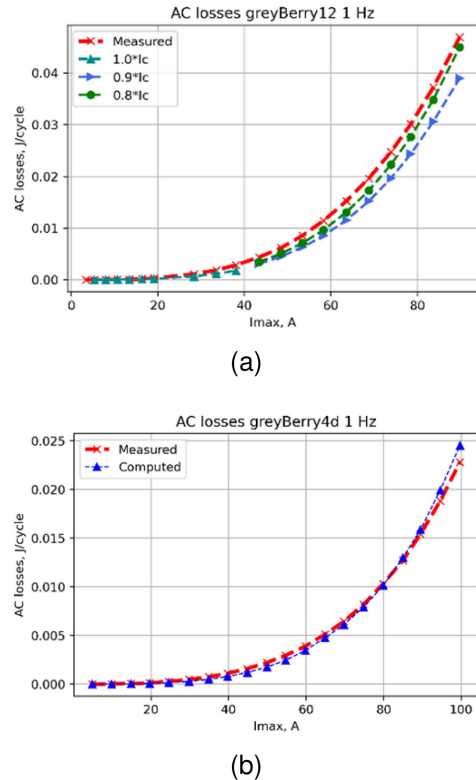


Fig. 7. Computed vs Measured AC losses per cycle of: (a) greyBerry12, (b) greyBerry4d.

#### V. CONCLUSION

This work presents the full development cycle—from conceptual design to computational modeling and experimental validation—focused on exploring REBCO soldered stack cables as a promising solution for high-field accelerator magnets.

We selected a straight, face-to-face soldered REBCO tape stack cable due to its high filling factor and ease of integration into racetrack-type coils, which are suitable for future demonstrator designs.

AC loss measurements were conducted at 77 K across a frequency range of 0.1 Hz to 20 Hz, with current amplitudes up to 100 A. The results showed that AC losses per cycle (J/cycle) remained nearly constant across the tested frequency range. Measured losses reached up to 25 mJ/cycle at 100 A for the 4-mm soldered stack coil, and up to 65 mJ/cycle at 100 A for the 12-mm single tape coil.

Both the 12-mm single-tape coil (greyBerry12) and the 4-mm face-to-face soldered stack coil (greyBerry4d) demonstrated excellent agreement with the FEM predictions, with discrepancies of less than 10%.

The developed method is simple for production of double-pancake coils and could find application for validation of losses different types of REBCO cables.

#### ACKNOWLEDGMENT

This work was performed under the auspices of and with support from the Swiss Accelerator Research and Technology (CHART) program ([www.chart.ch](http://www.chart.ch)).

## REFERENCES

- [1] B. Auchmann, "High field magnet programme–European strategy input," in *Proc. Workshop, CERN*, Geneva, Switzerland, Mar. 2025, pp. 3–4.
- [2] L. Rossi, "HTS accelerator magnet and conductor development in Europe," *Instruments*, vol. 5, 2021, Art. no. 8, doi: [10.3390/instruments5010008](https://doi.org/10.3390/instruments5010008).
- [3] T. Garg, J. Jaroszynski, E. S. Choi, M. D. Sumption, M. Majoros, and E. W. Collings, "Magnetization in ReBCO-Based CORC cables in magnetic fields up to 30 T for accelerator applications," *IEEE Trans. Appl. Supercond.*, vol. 35, no. 5, Aug. 2025, Art. no. 6603605, doi: [10.1109/TASC.2025.3540991](https://doi.org/10.1109/TASC.2025.3540991).
- [4] S. Kar, "Symmetric tape round REBCO wire with  $j_e$  (4.2 K, 15 T) beyond 450 Am $m^{-2}$  at 15 mm bend radius: A viable candidate for future compact accelerator magnet applications," *Superconductor Sci. Technol.*, vol. 31, 2018, Art. no. 059601, doi: [10.1088/1361-6668/aaba69](https://doi.org/10.1088/1361-6668/aaba69).
- [5] J. Fleiter, C. Lorin, and A. Ballarino, "On Roebel cable geometry for accelerator magnet," *IEEE Trans. Appl. Supercond.*, vol. 26, no. 3, Apr. 2016, Art. no. 4802805, doi: [10.1109/TASC.2016.2530872](https://doi.org/10.1109/TASC.2016.2530872).
- [6] B. Shen, F. Grilli, and T. Coombs, "Overview of H-formulation: A versatile tool for modeling electromagnetics in high-temperature superconductor applications," *IEEE Access*, vol. 8, pp. 100403–100414, 2020.
- [7] C. R. Vargas-Llanos, "Design and test of a setup for calorimetric measurements of AC transport losses in HTS racetrack coils," *Superconductor Sci. Technol.*, vol. 36, 2023, Art. no. 045015, doi: [10.1088/1361-6668/acbba5](https://doi.org/10.1088/1361-6668/acbba5).
- [8] "Faraday factory Japan," Product. Accessed: Oct. 13, 2025. [Online]. Available: <https://www.faradaygroup.com/en/product/>
- [9] "High-temperature superconducting wire critical current database." Accessed: Oct. 13, 2025. [Online]. Available: <https://htsdb.wimbush.eu/dataset/13708690>
- [10] F. Gömöry, "Voltage signals on the terminations of an HTS magnet modelled in A-T formulation," in *Proc. HTS 2024 Modelling Workshop*, Bad Zurzach, Switzerland, Jun. 2024, pp. 4–5.
- [11] J. Gerhold, "DC-Breakdown strength of liquid nitrogen under different voltage ramp conditions," in *Proc. 13th Int. Conf. Dielectric Liquids*, Nara, Japan, Jul. 1999, pp. 445–448.
- [12] J. ter Harmsel, "Magnetization loss and transport current loss in ReBCO racetrack coils carrying stationary current in time-varying magnetic field at 4.2 K," *Superconductor Sci. Technol.*, vol. 36, no. 1, 2023, Art. no. 015011, doi: [10.1088/1361-6668/aca83d](https://doi.org/10.1088/1361-6668/aca83d).
- [13] K. Zhu, "AC loss measurement of HTS coil under periodic current," *Physica C: Supercond. Appl.*, vol. 569, 2020, Art. no. 1353562, doi: [10.1016/j.physc.2019.1353562](https://doi.org/10.1016/j.physc.2019.1353562).
- [14] L. F. Goodrich, "Hysteresis in transport critical-current measurements of oxide superconductors," *J. Res. Nat. Inst. Standards Technol.*, vol. 106, no. 4, pp. 657–690, 2001, doi: [10.6028/jres.106.031](https://doi.org/10.6028/jres.106.031).
- [15] "Comsol Multiphysics software." Accessed: Oct. 13, 2025. [Online]. Available: <https://www.comsol.com/>
- [16] L. Bortot et al., "A coupled A–H formulation for magneto-thermal transients in high-temperature superconducting magnets," *IEEE Trans. Appl. Supercond.*, vol. 30, no. 5, Aug. 2020, Art. no. 4900911.
- [17] X. Ji, "The improved model based on the H-A formulation in large-scale HTS magnet," *Physica C: Supercond. Appl.*, vol. 618, Mar. 2024, Art. no. 1354431, doi: [10.1016/j.physc.2023.1354431](https://doi.org/10.1016/j.physc.2023.1354431).